Molecular Microbiology (2006) **59**(1), 67–83

doi:10.1111/j.1365-2958.2005.04928.x
First published online 24 October 2005

The polysaccharide capsule of the pathogenic fungus *Cryptococcus neoformans* enlarges by distal growth and is rearranged during budding

Oscar Zaragoza,[1] Andrew Telzak,[1] Ruth A. Bryan,[2] Ekaterina Dadachova[1,2] and Arturo Casadevall[1,3]*

Departments of [1]Microbiology and Immunology, [2]Nuclear Medicine and [3]Medicine, Albert Einstein College of Medicine, 1300 Morris Park Avenue, Bronx, NY 10461, USA.

Summary

The capsule of *Cryptococcus neoformans* can undergo dramatic enlargement, a phenomenon associated with virulence. A prior study that used Ab to the capsule as a marker for older capsular material concluded that capsule growth involved the intermixing of new and old capsular material with displacement of older capsular polysaccharide towards the surface. Here we have revisited that question using complement (C), which binds to capsular polysaccharide covalently, and cannot redistribute by dissociation and binding at different sites. The experimental approach involved binding of C to cells with small capsules, inducing capsule growth, and following the location of C relative to the cell wall as the capsule enlarged. C remained close to the cell wall during capsule growth, indicating that capsule enlargement occurred by addition of new polysaccharide near the capsule edge. This conclusion was confirmed by an independent method that employed radioactive metabolic labelling of newly synthesized capsule with ^{3}H-mannose followed by gradual capsular stripping with γ-radiation. Capsule growth proceeded to a certain size, which was a function of cell size, and was not degraded when the cells were transferred to a non-inducing medium. During budding, an opening appeared in the capsule of the mother cell that permitted the nascent bud to separate. Scanning EM suggested that a physical separation formed between the capsules of the mother and daughter cells during budding, which may avoid mixture between both capsules. Our results indicate that *C. neoformans* capsular enlargement also occurs by apical growth and that budding results in capsular rearrangements.

Accepted 23 September, 2005. *For correspondence. E-mail casadeva@aecom.yu.edu; Tel. (+1) 718 430 3665; Fax (+1) 719 430 8701. This paper is dedicated to the memory of Marshall Horwitz, great investigator and human being, and always an example to follow by everybody at the Albert Einstein College of Medicine.

Introduction

Microbial capsules are one of the great frontiers in cellular biology, because they are remarkably complex assemblies of polysaccharides that are poorly understood with regards to organization, architecture and structure. Many pathogenic prokaryotic microbes have polysaccharide capsules that are associated with virulence. *Cryptococcus neoformans* is the only encapsulated microbe among eukaryotic pathogens (for review, see Casadevall and Perfect, 1998). The capsule of *C. neoformans* is the most distinctive physical structure of the cryptococcal cell, and can be easily visualized as a halo surrounding the yeast cell when the microbe is suspended in Indian ink. For *C. neoformans*, the capsule is believed to increase microbial fitness in both the environment and during mammalian pathogenesis (Casadevall and Perfect, 1998). In the environment, the *C. neoformans* capsule may protect the fungus against amoeboid and nematode predators (Steenbergen *et al*., 2001). During infection, the *C. neoformans* capsule contributes to virulence by promoting the intracellular survival of cryptococci after ingestion by macrophages (Feldmesser *et al*., 2000a; Tucker and Casadevall, 2002). The *C. neoformans* capsule has antiphagocytic properties (Mitchell and Friedman, 1972; Kozel and Gotschlich, 1982; Kozel *et al*., 1988), and elicits a poor antibody response (Murphy and Cozad, 1972; Kozel *et al*., 1977). Furthermore, capsular polysaccharide is released during the course of infection and is believed to interfere with the generation of effective immune responses through a variety of mechanisms. These mechanisms range from altered regulation of cytokine responses to interference with antigen presentation (Vecchiarelli, 2000).

Relatively little is known about the structure of the assembled capsule. Much of the available information on its composition and structure is inferred from analysis of shed polysaccharide released into the culture medium during *in vitro* growth. The capsule has at least three

components: glucuronoxylomannan (GXM), galactoxylomannan and mannoprotein (Cherniak and Sundstrom, 1994). The major component, GXM, consists of an unbranched mannose backbone with varying amounts of xylose, glucuronic acid and O-acetyl substitution. Construction of the capsule requires the formation of GDP-mannose, UDP-xylose and UDP-glucuronic acid (for review, see Doering, 2000; Bose *et al*., 2003). Several enzymes involved in this process have been cloned and characterized (Bar-Peled *et al*., 2001; 2004; Sommer *et al*., 2003). In addition, several genes named *CAP* genes have been isolated by complementation of capsule-deficient mutants (Chang and Kwon-Chung, 1994; 1998; 1999; Chang *et al*., 1996), but the biochemical function and the role of these genes in capsule construction is not known. One gene, *CAP59*, appears to be involved in the trafficking of the polysaccharide from intracellular synthesis sites to the space where the capsule is presumably assembled (Garcia-Rivera *et al*., 2004). Recent reports indicate that attachment of the capsular polysaccharide depends on the α-1,3-glucan of the cell wall (Reese and Doering, 2003). The porosity of the capsule varies depending on its radius, being higher at the edge, and lower near the cell wall (Gates *et al*., 2004). In addition, the density of the capsular polysaccharide matrix is higher in cells isolated from infected animals (Gates *et al*., 2004). A comparison of antigenic composition between *in vivo* and *in vitro* capsules revealed organ-related differences suggesting evolution of capsule structure during infection (Charlier *et al*., 2005). Acetylation is also an important factor responsible for the immunogenic and virulent properties of the capsule (Moyrand *et al*., 2002; Kozel *et al*., 2003; McFadden and Casadevall, 2004).

After mammalian infection, the capsule undergoes a significant increase in size (Bergman, 1965; Cruickshank *et al*., 1973; Love *et al*., 1985; Rivera *et al*., 1998; Feldmesser *et al*., 2001). Several stimuli, such as high CO_2 levels, iron limitation and serum, induce capsule growth *in vitro* (Granger *et al*., 1985; Vartivarian *et al*., 1993; Zaragoza *et al*., 2003a). Several new capsule-inducing conditions have recently been identified, including nutrient deprivation and alkaline pH (Zaragoza and Casadevall, 2004). Capsule growth interferes with complement (C)-mediated phagocytosis through a mechanism whereby capsule-bound C3 is inaccessible to the C receptor (Granger *et al*., 1985; Zaragoza *et al*., 2003b). Understanding the mechanism of capsule growth in *C. neoformans* is important because the transition from a small to a large capsule occurs during animal infection, and the phenomenon is also associated with virulence. To approach this problem, it is necessary to label the old polysaccharide in a cell while not interfering with viability such that capsule growth is possible. The one prior study that addressed this problem used antibody to label the older capsular polysaccharide (Pierini and Doering, 2001). That study concluded that new and old polysaccharide mixed during capsule growth. However, as antigen–antibody reactions are potentially reversible, the suitability of Ab as a stable marker of capsular geography is uncertain. In this study, we have revisited that problem using C labelling. Unlike polysaccharide–antibody interactions, C binds to the capsule by a covalent thioester bond that is not prone to dissociation (Kozel *et al*., 1984; 1989; 1992; Kozel and Pfrommer, 1986). Using C labelling, we now demonstrate that the old capsular material remains located close to the cell wall during capsular enlargement, and does not migrate to the outside. The results suggest a different model for capsule growth and rearrangement during the dynamic transformations that accompany capsular enlargement and budding.

Results

Dynamics of capsule growth

To study the dynamics of capsule growth, it is necessary to label the initial capsule with a marker that allows visualization without impairing cellular viability or interfering with capsular growth. We first evaluated the suitability of Ab as a landmark for capsule growth studies in *C. neoformans*. As the binding of the Ab to the capsular polysaccharide is not covalent, the Ag–Ab complex could potentially dissociate and reform at another site in the capsule. If this occurred, the location of Ab would change depending on the size of the capsule and the incubation time. To test this possibility, cells with large capsules, generated by serum induction of capsule growth, were labelled with mAb, washed, and then incubated with unlabelled small capsule cells. The reverse experiment was also done whereby cells with small capsule were labelled with Ab and incubated with large capsule cells. In this experiment, capsule size was used to distinguish between cells initially labelled with mAb, and we established that there was no change in capsule size or fungal replication during experimental conditions. When Ab-labelled large or small capsule cells are mixed with small or large capsule cells respectively, there was a redistribution of the Ab, such that at the completion of the experiment all cells were Ab-stained (Fig. 1A–F). We performed this study with two mAbs, 18B7 and 2H1, that differ in apparent affinity for GXM. In the case of mAb 18B7, the signal observed in the unlabelled cells corresponding to Ab-redistribution was much lower than in the case of mAb 2H1 (data not shown). This was consistent with the fact that the apparent affinity of mAb 18B7 is 10-fold greater than that of 2H1 (Mukherjee *et al*., 1993). After the incubation, the proportion of cells with small and large capsules was the same, ~50% each. This indicated that there was no significant

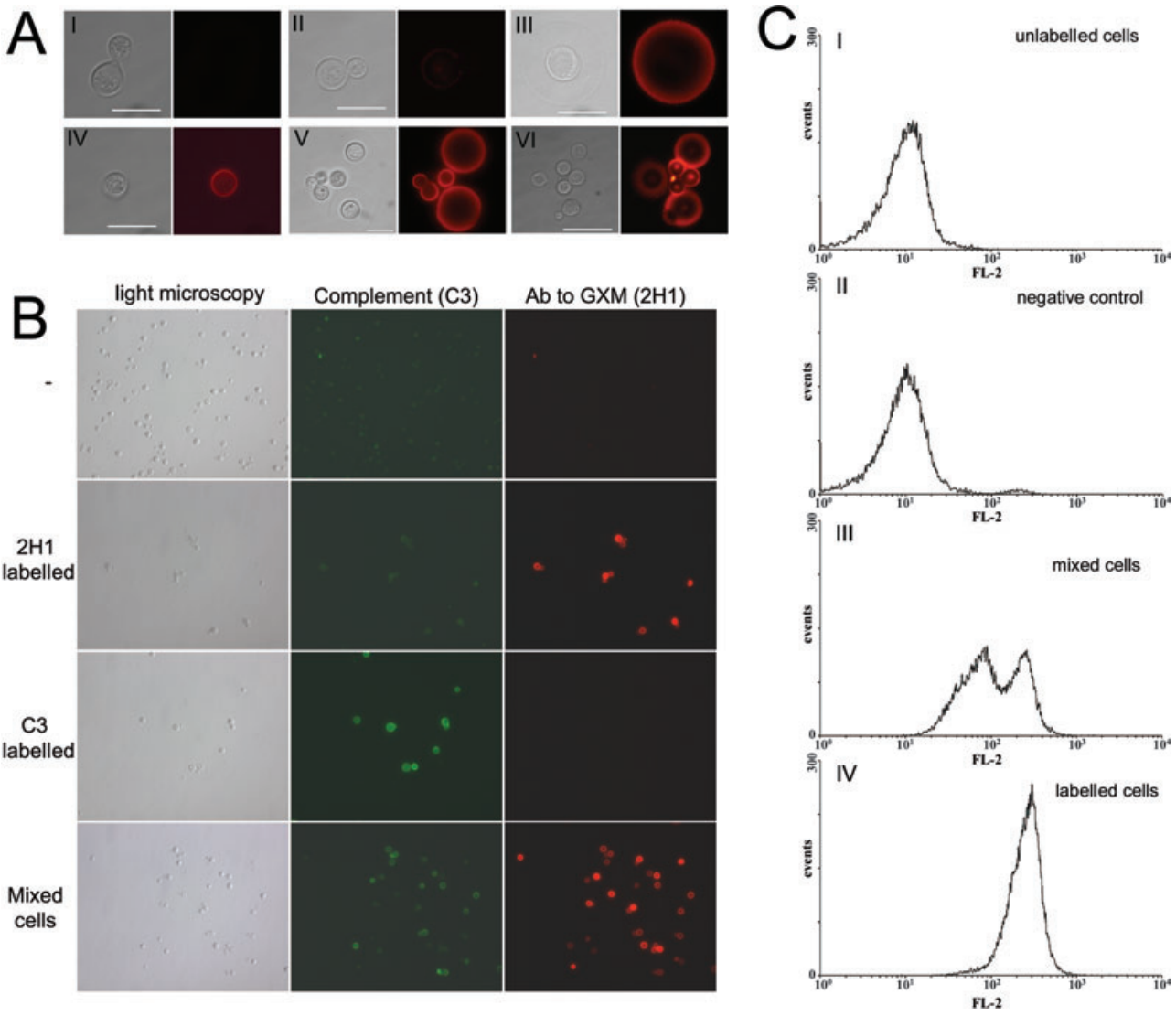

Fig. 1. Ab exchange experiments between cells. (A) Labelling of the cells with mAb 2H1; (B) labelling of one population with C and other with mAb 2H1 and analysis by immunofluorescence; (C) analysis by FACS.
A. Cells with small or large capsules were labelled with mAb 2H1 (10 μg ml^{-1}) for 1 h at 37°C, and then mixed with unlabelled cells of different capsule size. Parallel samples without labelling were carried out, and incubated in the last wash of the labelled cells, to rule out that the signal detected originated from Ab left in the medium. The cells were mixed and incubated overnight at 30°C. Then, Ab was detected with a goat anti-mouse IgG TRITC conjugated Ab. (I) Large capsule cell, unlabelled; (II) Small capsule cell, unlabelled; (III) large capsule, labelled; (IV) small capsule, labelled; (V) large capsule labelled mixed with unlabelled small capsule; (VI) small capsule cell labelled mixed with unlabelled large capsule cell. Left panel, light microscopy, right panel, rhodamine fluorescence. Scale bars denote 10 microns.
B. Cells with small capsule were labelled with 2H1-Alexa 488 conjugated mAb (1 μg ml^{-1}), and cells with large capsule were incubated in serum to allow C deposition. After the labelling, the cells were mixed overnight as in A, and both mAb and C were identified by fluorescence.
C. FACS experiment. H99 cells were heat killed and then kept in PBS (I), or incubated with a 2H1-Alexa 488 conjugated mAb (2 μg ml^{-1}) (IV). The cells were washed, and the last wash of the labelled cells were used to incubate unlabelled cells as negative control (II). After the wash, samples of labelled and unlabelled cells were mixed (III). All the four samples were incubated overnight at 37°C and analysed by FACS. The graphs represent fluorescence intensity (FL-2 channel, *x* axis) versus number of cells counted (events, *y* axis).

growth during the overnight incubation in PBS, as expected from prior studies (Steenbergen *et al.*, 2001). In addition, we carried out controls where cells were incubated alone overnight without mixing and noted no significantly change capsule size. The possibility that the uniform labelling was caused by an artifact of incomplete washing, such that some Ab was left after washing, was also ruled out, because incubation of the last wash solution with unlabelled cells resulted in no Ab labelling (Fig. 1A). When this experiment was performed using C, instead of Ab for labelling cells, we did not observe any exchange of label between the cells (Fig. 1B). For that

experiment, we labelled cells with small capsule with mAb 2H1 and cells with large capsule with C, and mixed them as before. After the overnight incubation, we observed that mAb distributed between all the cells, while C did not. This showed that the initially C-labelled small or large capsule cells retained the same label at the end of the experiment, and there was no transfer of C to unlabelled cells. In contrast, mAb 2H1 redistributed between cells. These results are consistent with the fact that Ag–Ab interactions are non-covalent and potentially reversible depending on conditions, while C-polysaccharide interactions maintained by covalent bonds and are essentially irreversible.

To confirm that Abs bound to the cryptococcal capsule could dissociate and reassociate with unlabelled cells by a secondary method that would permit analysis of a larger number of cells, we designed a FACS experiment. In that experiment, we employed heat-killed cells with small capsule to avoid any concern about cell division. Cells were labelled with mAb 2H1 conjugated to Alexa (Feldmesser *et al.*, 2000b) and incubated overnight with unlabelled cells. We used the same concentration of cells and mAb as used by Pierini and Doering (2001) to make sure that binding of mAb occurred in a similar manner as described in the prior study. We analysed labelled and unlabelled cells as positive and negative controls respectively. Moreover, we kept the supernatant from the last wash and incubated unlabelled cells in this solution, to make sure that there was not sufficient Ab left unbound after the last washing that could bind to the unlabelled cells. As shown in Fig. 1C, the FACS analysis of unlabelled and labelled cells revealed, as expected, two different peaks of fluorescence. After mixing the cells, the peak of the negative cells was displaced to the right. This was a result of an increase in the fluorescence caused by mAb migrating from the previously labelled cells to the unlabelled cells. Unlabelled cells incubated with the last wash solution gave the same profile as the negative control, ruling out incomplete washing as an explanation for this effect. The same result was obtained using different concentrations of mAb (1 or 2 $\mu g\ ml^{-1}$). This experiment confirms that the binding of mAbs to the capsule is reversible. Consequently, mAb is not a stable marker for the study of capsule growth.

Establishing the suitability of C staining as a capsule marker required validating that it bound to the capsule, and not to the cell wall, because the latter would remain fixed during any capsular enlargement. To investigate this possibility, H99 cells were incubated with C, and then stained with calcofluor dye, which binds to the cell wall. This experiment showed that the fluorescence signal due to C and calcofluor did not colocalize, thus establishing that the C was bound to the capsule and not to the cell wall (Fig. 2A). The differences in the localization of C and calcofluor could be explained by C binding to the capsule and calcofluor binding to the cell wall, or C binding to a different region of the cell wall than calcofluor. To discard this last possibility, we measured the thickness of calcofluor signal and the thickness of the cell wall measured by light microscopy, and found both measurements were identical, indicating that calcofluor does not bind to an inner region of the cell wall (result not shown). Furthermore, the distance between the calcofluor staining and C staining area was much greater than either the calcofluor or cell wall thickness providing a powerful geometrical argument for C binding to the capsule in the encapsulated strain. This result further supports our contention that C binds to the capsule. In addition, cells with enlarged capsule deposited C in a location that was clearly away from the cell wall, in the middle region of the capsule (see Fig. 7A). Furthermore, the pattern of C immunostaining in encapsulated cells had a fuzzy edge, and differed from the defined thick line expected from C binding to cell wall, as evident following C binding to the acapsular *cap67* mutant (Fig. 2B, compare C labelling with Fig. 2A in both cases). Fuzziness in C immunostaining of encapsulated cells is consistent with binding to the capsule, and suggests that C binds to different places in encapsulated and acapsular strains. In the acapsular cells, both signals practically overlapped, consistent with calcofluor binding to the cell wall and C binding to the cell surface. Furthermore, if C binds to the capsule, protocols that promote the release of polysaccharide from the capsule should also release C. γ-radiation of cryptococcal cells can strip the cells of their capsules (Bryan *et al.*, 2005). Hence, we coated cells with C, and irradiated them. As shown in Fig. 2C, radiation completely released C from the cells of a wild type strain. However, it had no effect when C was bound to the acapsular mutant *cap67*, where the absence of capsule produces direct binding to the cell wall, because there is no capsule to interfere with binding. This result confirms that C binds to the inner part of the capsule in encapsulated cells and not to the cell wall.

After establishing the suitability of C as a geographical marker for capsule growth studies, we employed C labelling to study capsular growth dynamics. When cells were labelled with C and capsule growth was induced, C remained localized deep in the capsule, close to the cell wall. This result implies apical capsular growth and is not consistent with a model of capsule growth whereby all capsular material from the inner layers of the polysaccharide capsule migrates outward during capsular enlargement.

To ensure that the different results observed using C and Ab as markers were not due to inter-laboratory differences (such as strain stock, growing media, etc.), we reproduced the experimental findings of the prior study (Pierini and Doering, 2001) using mAb as a capsule marker with directly labelled mAb 2H1-Alexa488 (data not

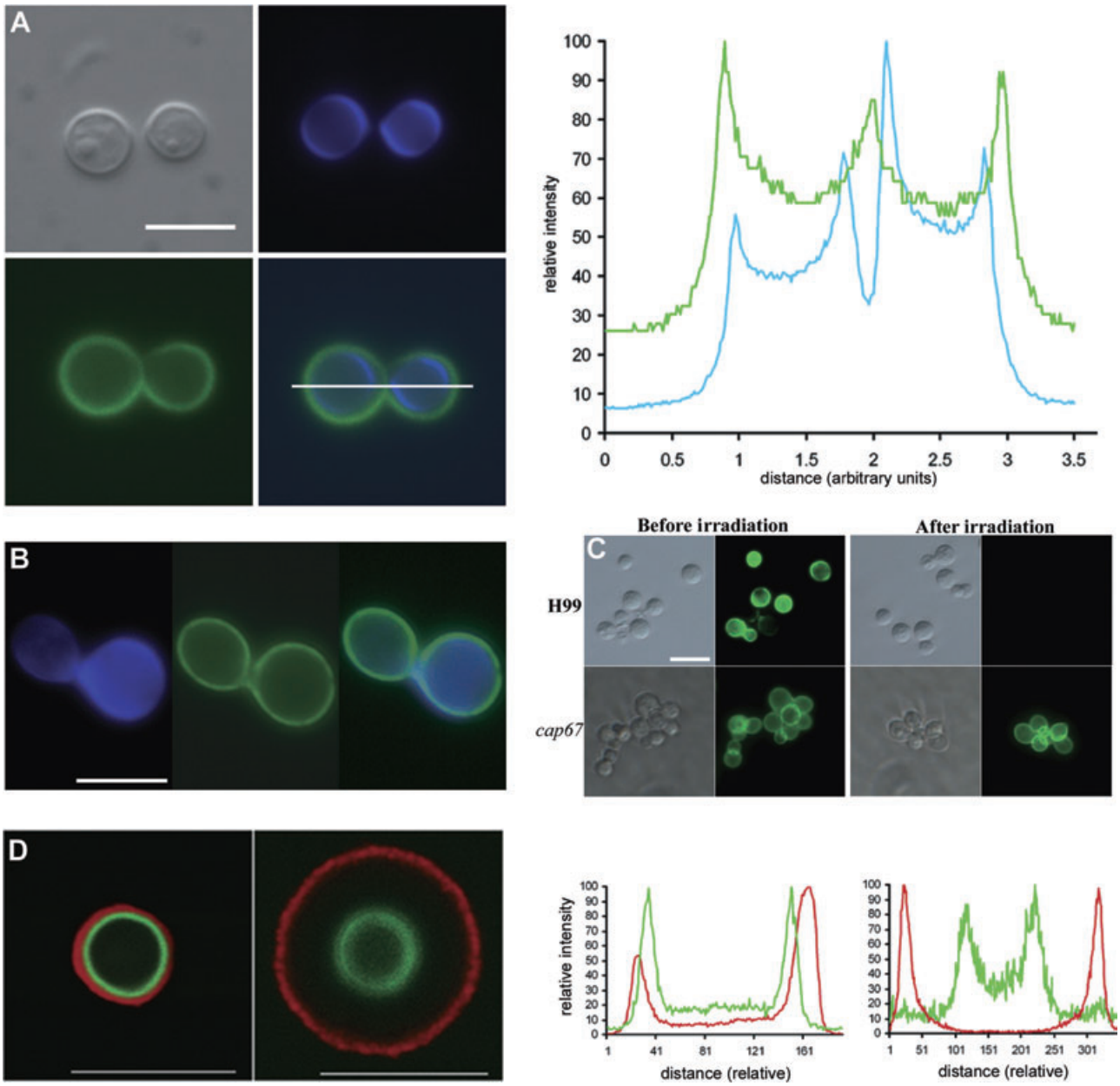

Fig. 2. Mode of growth of the capsule using C as a marker.
A. Complement does not bind to the cell wall. H99 cells were grown in Sabouraud medium, and C labelled by incubation in serum for 1 h at 37°C. Then the cells were washed and incubated with goat anti-mouse complement FITC conjugated Ab in PBS containing calcofluor white to label the cell wall. Upper left panel, light microscopy; upper right, calcofluor, lower left, complement, lower right, merge. Scale bar, 10 μm. Fluorescent intensities profiles (right diagram) were obtained with ImageJ software.
B. Cells from *cap67* mutant grown in Sabouraud medium, and labelled with C as in A. C and cell wall were detected as in A. Scale bar, 5 μm.
C. γ-radiation of H99 and *cap67* C-coated cells. H99 and *cap67* strain were incubated in mouse serum to allow C deposition, then suspended in PBS and exposed to γ-radiation to release the capsule. After the irradiation, C was detected by immunofluorescence as described in *Experimental procedures*. Scale bar in first panel, 10 μm, and applies for the rest of panels.
D. Complement localization before and after capsule growth. Cells with small capsule were incubated in serum for 1 h at 37°C. Then the cells were washed and placed in PBS + 10% heat inactivated FCS overnight at 37°C. Then the capsule was detected adding mAb 18B7 and goat anti-mouse IgG1-TRITC conjugated, and C with a goat anti-mouse complement FITC Ab. Pictures were taken with a Bio-Rad Confocal microscope. Panels show the merge for both rhodamine and fluorescein signals. Bar denotes 10 microns. The intensities profiles at the right part of the figure denote the fluorescence as a function of cell radius before (left) and after (right graph) capsule induction.

shown). In addition, we also carried out a double labelling experiment, in which cells with small capsule were labelled with both mAb and C, and then capsule growth was induced. In this experiment, we obtained the same result, redistribution of the mAbs through the capsule, while C stayed in a location close to the cell wall (results not shown), thus confirming that the differences observed were not due to inter-laboratory differences.

As C does not label the entire capsule, we used an independent method to ascertain the validity of our conclusions involving metabolic labelling and gradual stripping of the outer capsule with γ-radiation, which removes the outer capsule (Bryan *et al*., 2005). We hypothesized that if our conclusions from the C staining studies were correct, the capsule material induced in conditions of radioactive metabolic labelling would result in radioactivity incorporation in the outer capsule. As γ-radiation removes the outer capsule, the material released initially from metabolically labelled cells should have the highest cpm per amount of polysaccharide. Hence, we incubated cells with ^{3}H-mannose, induced capsule growth, carried out gradual stripping of capsule layers with γ-radiation and measured radioactivity in the released polysaccharide as a function of irradiation time (7, 20 and 40 min) and polysaccharide amount. Consistent with our prior study (Bryan *et al*., 2005), the amount of polysaccharide released after 20 min was much greater than the amount released after 7 min, which also correlated with a decrease in capsule size (Fig. 3B and C). However, when we measured the radioactivity released and correlated the cpm with the amount of polysaccharide, the highest ratio was measured for polysaccharide released after a short irradiation time. In fact, the polysaccharide released after long irradiation times had significantly lower cpm per polysaccharide implying that most of the polysaccharide in the interior of the capsule was not radioactively labelled. To exclude the possibility of non-specific incorporation of the mannose to the capsule, we did the same experiment with heat-killed cells, and observed no incorporation at all, which excludes the possibility of non-specific binding of ^{3}H-mannose to the capsule (result not shown). To confirm that radioactivity was incorporated into GXM, we incubated the supernatants obtained after the radiation with sepharose conjugated with the mAb to GXM 18B7, and observed that most of the radioactivity was retained by the sepharose matrix (result not shown). This result indicated that most of the radioactive mannose was incorporated into GXM, a finding consistent with previous report that mannose is incorporated directly into GXM (Cherniak *et al*., 1998).

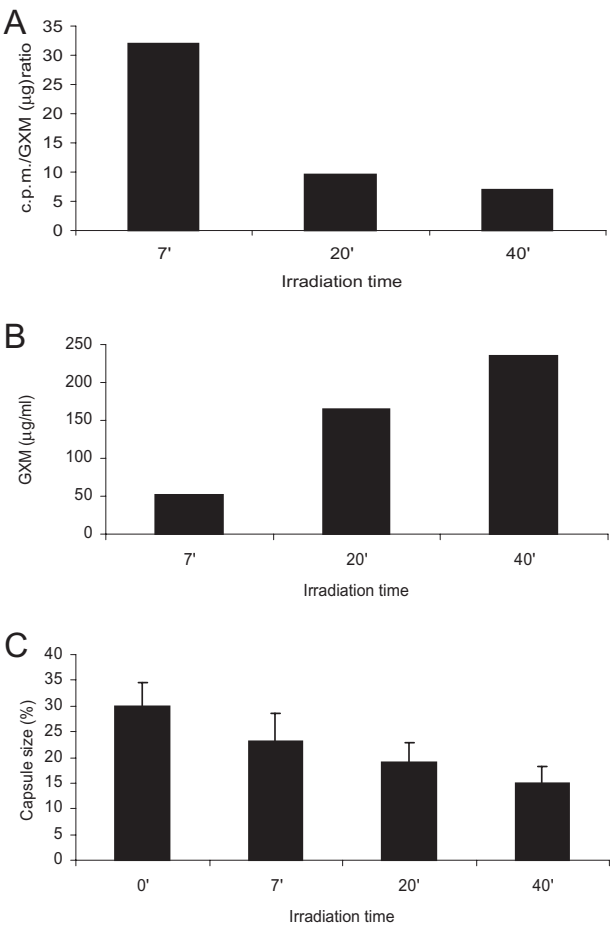

Fig. 3. Radioactive labelling of the capsule with ^{3}H-mannose and analysis after γ-radiation. Cells from H99 strain grown in Sabouraud were incubated with 50 μCi of ^{3}H-mannose for 3 h. Then the cells were irradiated with γ-radiationfor 0, 7, 20 and 40 min, and both the amount of radioactivity and capsular polysaccharide released in the supernatant were measured in an scintillation counter or by capture ELISA. The amount of polysaccharide released (A) and the ratio of radioactivity/polysaccharide (B) are plotted. The experiment was repeated twice obtaining the same result. (C) Capsule size was measured in parallel after irradiating the cells as described in *Experimental procedures*. The mean value and the standard deviation are plotted.

The limits of capsule growth

Given that *C. neoformans* cells in tissue often manifest different sized capsules, we wanted to establish the limits of capsule growth in relation to time and nutrient availability. To investigate these variables, we transferred the cells several times through inducing medium containing a limited amount of nutrients (Sabouraud medium diluted 10 times in MOPS 50 mM pH 7.3), because capsule growth was consistently enhanced in this medium (Zaragoza and Casadevall, 2004). After the second passage we noted that the size of the capsule did not increase further. This result implies that once capsule enlargement reaches a certain size, prolonged exposure to inducing medium does not promote further capsule growth (Fig. 4A).

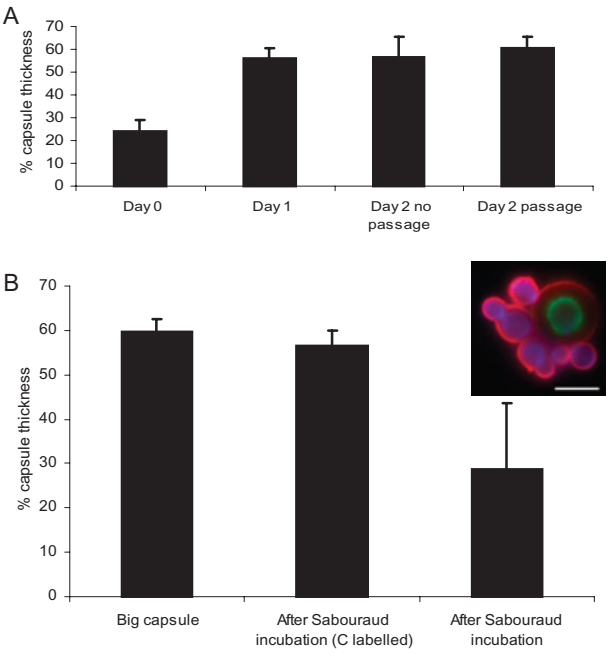

Fig. 4. Dynamics of capsule growth and decrease.
A. Capsule growth after several passages through inducing medium. Cells from H99 strain were grown overnight in Sabouraud medium (day 0) and relative capsule size was determined as described in *Experimental procedures*. Capsule growth was then induced overnight by placing the cells in 10% Sabouraud in MOPS 50 mM pH 7.3. After the first induction (day 1), capsule size was determined again, and the cells were separated in two aliquots. One of them was kept in the same medium (day 2 no passage), and the other aliquot was centrifuged and placed in fresh inducing medium (day 2, passage). Both samples were incubated overnight at 37°C, and capsule size was determined after the second induction. The mean value and the standard deviation are represented in the graph.
B. Dynamics of capsule size decrease. Capsule size of H99 strain was induced by placing the cells in 10% heat-inactivated FCS overnight. Capsule size was determined by placing the cells in Indian ink (bar labelled as big capsule). Then the cells were labelled with C by incubating the cells in mouse serum for 1 h, and placed Sabouraud medium overnight. Then, capsule edge, C and cell wall were detected by immunofluorescence using mAb to the capsule 18B7 and goat anti-mouse IgG1-TRITC, goat anti-mouse complement FITC and calcofluor respectively. Panel in the upper right show a representative field with cells labelled with C and non-C labelled. These latter cells are presumably new cells generated during the growth period (scale bar, 10 μm). Using these markers, capsule size was calculated in cells labelled with C (bar labelled as After Sabouraud incubation C labelled) and in the whole population of cells, with and without C labelling (bar labelled as After Sabouraud incubation). The mean value and standard deviation are represented.

The capsule of C. neoformans *does not decrease in size once it has been enlarged*

We investigated whether cells with large capsules could reduce their capsule size when placed in conditions associated with the emergence of small-capsule cells. Our prior studies had suggested that capsular enlargement in media containing serum was associated with slower cell growth (Zaragoza *et al*., 2003a; Zaragoza and Casadevall, 2004), a finding which may be interpreted to suggest that re-insertion of cells with large capsules into rich nutrient conditions may reduce capsule size. To study the kinetics of capsular remodelling once faster growth resumed, we induced the size of the capsule in diluted Sabouraud medium (Zaragoza and Casadevall, 2004), then labelled cells with C, which does not segregate to the bud (see sections below), and induced rapid growth by transferring to Sabouraud medium. After 24 h of growth in the non-inducing medium, most of the cells in the culture had small capsules. When we measured the size of the capsule of the cells labelled with C, we observed no difference between the size of the capsule of these cells and those of the cells which had originally been placed in this medium prior to capsule growth induction (Fig. 4B).

Correlation between capsule size and cell size

As the enlargement of the capsule is a controlled process, and our experiments suggest that it is not degraded once induced, we explored whether capsule size was related to cell size. Consequently, we selected the cells for which larger capsules were induced in the presence of serum (cells from Fig. 4A and B), and plotted the size of the capsule versus the size of the cell. We calculated lineal diameter, surface and volume of both structures. For each of these parameters there was a positive correlation with the size of the capsule (Fig. 5).

Expression of CAP *genes during capsule growth induction*

Several genes have been shown to be required for the presence of the capsule phenotype, and we investigated whether capsular enlargement was associated with changes in the expression of these genes. Hence we collected cells from various capsule growth conditions, and measured the expression of four *CAP* genes (*CAP10*, *CAP59*, *CAP60*, *CAP64*) by real-time polymerase chain reaction (PCR). We did not find any significant change in the expression of these genes (result not shown).

Capsule rearrangements during budding

We observed that once the capsule is induced by serum, budding was accompanied by changes in the structure of the capsule. During budding, the capsule often lost its well-rounded shape in the area where budding occurred, and the transit of a new cell through the capsule of the mother cell was usually accompanied by an invagination of the capsule surface at the site of budding (Fig. 6A–C). This appeared to facilitate the emergence of the bud closer to the edge of the capsule. This observation is consistent with, and confirms prior findings, which showed Indian ink penetration at the region of budding (Pierini and Doering, 2001). We observed similar rearrangements in

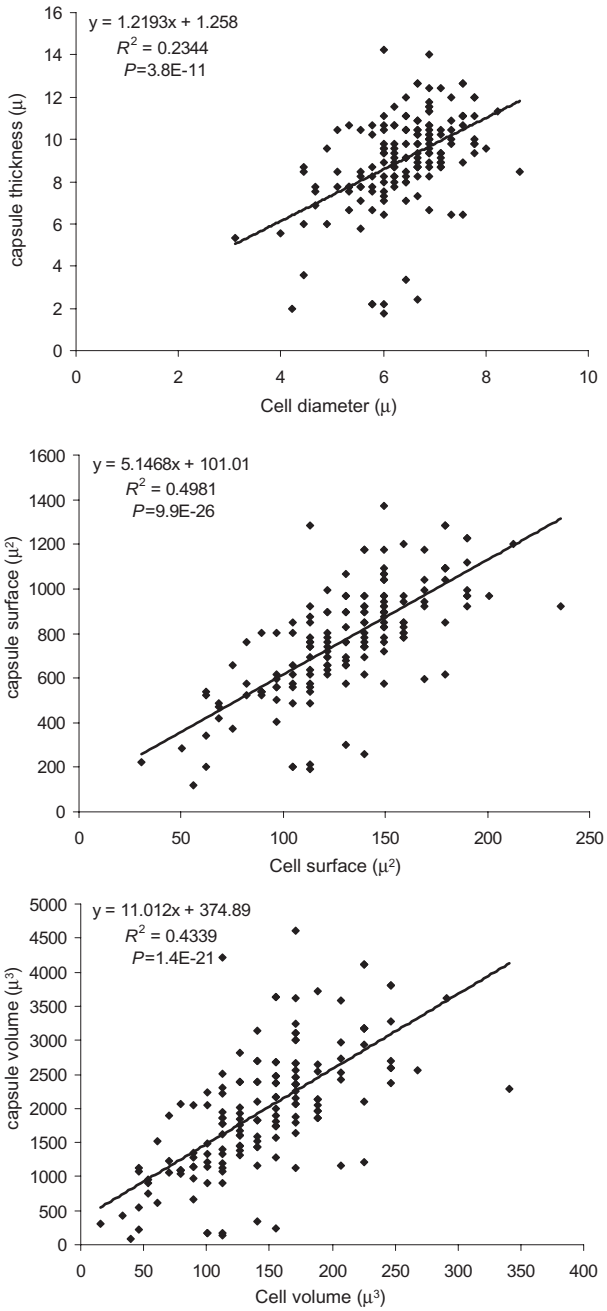

Fig. 5. Correlation between capsule size and cell size. The volume of the capsule and cell body from the cells whose capsule was induced in serum in Fig. 4A and B was plotted and correlated. The equation of the formula and the R^2 value are shown, and *P*-value was calculated using Pearson test.

budding cells in which the capsule was visualized by immunofluorescence (Fig. 6D). This sequence of events suggested that budding and separation of the bud from the mother cell required capsular degradation and/or reorganization.

We applied the C labelling technique to study the capsular rearrangements accompanying budding. Cells were first arrested in growth by incubation in capsule-inducing medium for 3 days, and then incubated in serum to allow C deposition on the capsule. Finally the cells were induced to divide by transferring to Sabouraud media. Then we recorded images at several times, and observed the change in C localization at different stages of budding. We observed that replication was associated with a loss of staining at the site of budding, and a tunnel formed in the capsule to allow the migration of the bud (Fig. 7A). Interestingly, when the bud was already separated from the mother cells, we noticed that the fluorescence was again present in the capsule of the mother cells in the area of budding. These changes in C localization could be observed at very early stages of budding (Fig. 7B). When cells were labelled with C and allowed to bud, changes in C signal were apparent when the mother cells began the typical morphological changes in the cell wall, which included the appearance of a tip at the place where new bud emerges (Fig. 7B). The images suggest that at the moment of budding, a tunnel forms in the capsule of the mother cell that allows the efficient separation of the bud and the capsule of the mother cell, while not allowing their capsules to mix in the process. Similar findings were obtained when the capsule was labelled with mAb (Fig. 8A). It is striking that, despite the fact that an Ab can change its location from cells with small and large cap-

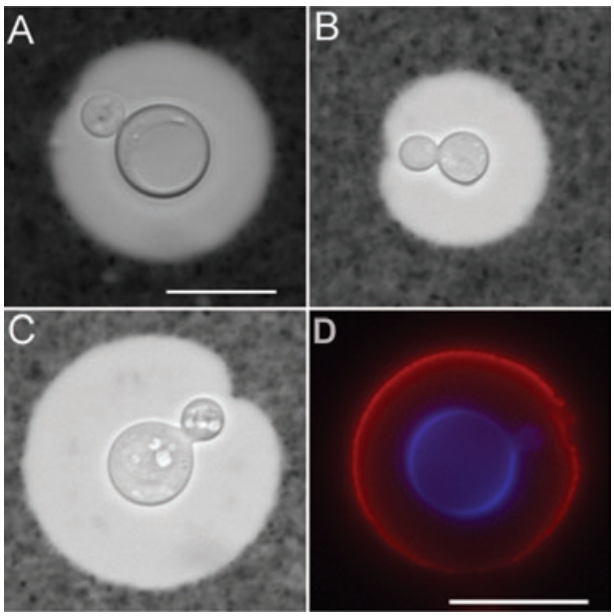

Fig. 6. Invagination of the capsule in the budding area. Capsule size of several *C. neoformans* strains was induced by placing the cells in PBS + 10% FCS for 3 days, and budding was induced by transferring the cells to Sabouraud medium for 3 h. A–C. Indian ink; D. fluorescence pattern. Strains (A), 24067 (B), H99 (C), 102.7. (D) H99 strain, capsule detected by immunofluorescence, using mAb 18B7 and goat anti-mouse IgG1-TRITC. Cell wall was detected with calcofluor. The picture shows the merge of light from the various fluorescence reporters. Scale bars denote 10 μm (bar in A applies for B and C).

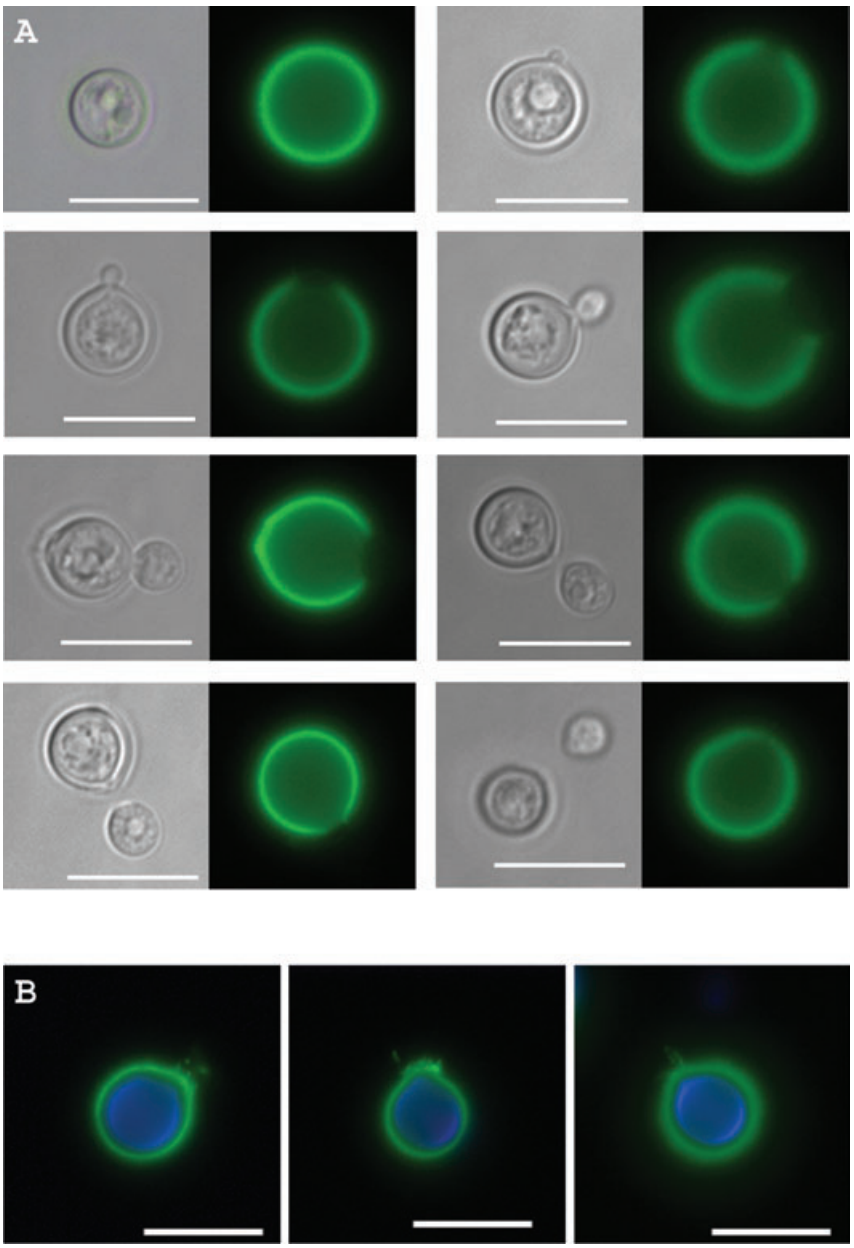

Fig. 7. Rearrangements of the capsule during budding monitored by C. Capsule size was induced to enlargement by placing the cells in PBS + 10% FCS during 3 days. The cells were then incubated in mouse serum to label the capsule with C, and budding was induced by placing the cells in fresh Sabouraud medium.
A. Pictures were taken at 2, 4, 8 or 24 h, and several cells in different stages of budding were photographed. Complement was detected by immunofluorescence using a goat anti-mouse complement FITC conjugated Ab. Left panel, light microscopy; right panel, complement (green fluorescence). Scale bars denote 10 microns.
B. Cells which capsule size has been enlarged were labelled with C as in A, and pictures were taken after 2 h of incubation in Sabouraud. Cells in which the mother cell has changed the morphology and the place where the bud is going to emerge are shown. Complement was detected as in A, and cell wall was detected with calcofluor. Scale bars, 10 μm. Three different representative cells are represented.

sules when they are co-incubated (see above), Ab does not bind to the bud. This phenomenon may reflect either the rapid kinetics of the budding process relative to Ab equilibration phenomena, or imply the existence of a mechanism that prevents mixing of the capsules from the mother cell and the bud. To ensure that the structure of the capsule of the bud allows binding of Ab, we incubated budding cells with mAb to the capsule, and observed that this capsule bound mAb efficiently (Fig. 8B).

The fact that neither pre-bound C nor Ab are found in the bud indicates that there is a mechanism that avoids the mixture of material between the capsule of the mother cell and the bud, and implies that the polysaccharide of the bud is newly synthesized. Given that light microscopy observations suggested that a tunnel formed in the capsule of the mother cell during budding, which presumably precluded mixing of parental and daughter cell capsular material, we used scanning electron microscopy (EM) to visualize this phenomenon. The images from scanning EM revealed a separation of the capsule between the mother and daughter capsules at the site of budding, and deep depressions in the capsule of the mother cell consistent with tunnel formation in the mother capsule during budding. Furthermore, we noted that in the bud, the region closest to the mother cell had a much lower amount of polysaccharide attached to the capsule, suggesting that

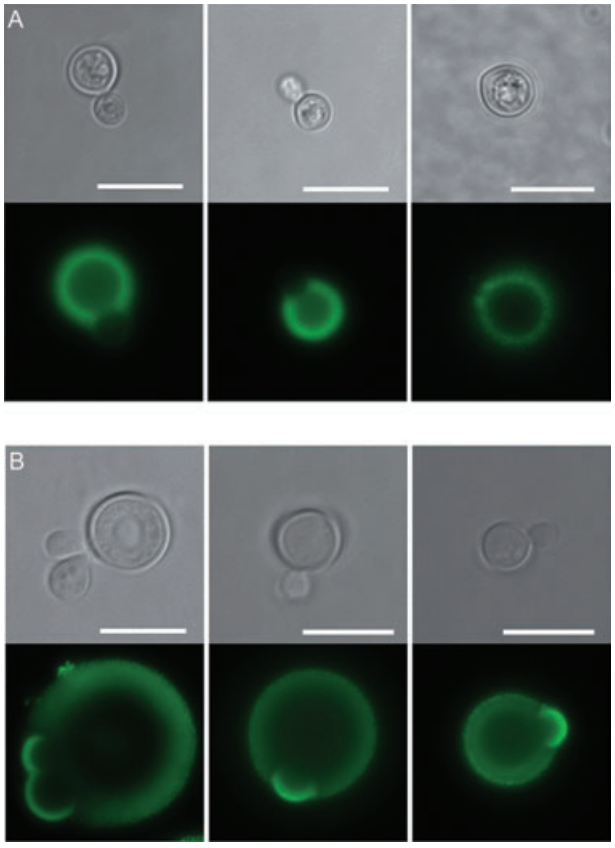

Fig. 8. Rearrangements of the capsule during budding monitored by Ab labelling.
A. Capsule size was increased as in the legend of Fig. 7, and the cells were labelled with mAb FITC conjugated mAb 2H1. Budding was induced by placing the cells in fresh Sabouraud medium. Three different cells are represented. Upper row, light microscopy; lower row, fluorescence.
B. Budding of cells with big capsule was induced as described in *Experimental procedures*. After 4 h of incubation, the cells were incubated with mAb 2H1 FITC conjugated. Upper row, light microscopy; lower row, fluorescence. Scale bars in all the pictures denote 10 μm.

the new capsule was probably synthesized beginning in the tip of the cell (Fig. 9A). It is possible that in this area between the mother cell and the bud, there is no polysaccharide attached, and that the few fibres observed are the consequence of collapse of polysaccharide from adjacent areas during the dehydration of the cells for EM. This suggests that the synthesis of polysaccharide in the bud begins from the distal tip of the bud, and expands in the direction of the mother cell. The idea of a physical separation was supported by the pattern of C deposition in budding cells (Fig. 9B). When the bud is still close to the mother cell, C labelling was uniform and continuous, but when the bud was about to leave the capsule of the mother cell, the labelling was not continuous. There was no labelling in the bud tip close to the mother cell, suggesting that the capsule of the bud is not complete in this area. At the same time, we observed that C was able to bind in the capsule of the mother cell, which suggests that the mother cells repair the hole produced in the capsule shortly after the daughter cell separates.

Discussion

We have re-examined the dynamics of capsular rearrangements during *C. neoformans* capsule and cell growth using new techniques, and obtained evidence suggesting the need to revise current concepts of capsular remodelling. A previous study using Ab to label capsule had concluded that addition of new polysaccharide to the capsule occurred in the inner part of the capsule, with the new material displacing the old polysaccharide to the edge of the capsule. In this study, we have established that an Ab bound to a cryptococcal capsule can dissociate and transfer to other cells. This result indicates that Ab is not a stable marker for polysaccharide capsular geography, and consequently, is not optimal for studying the capsular rearrangements that accompany capsule

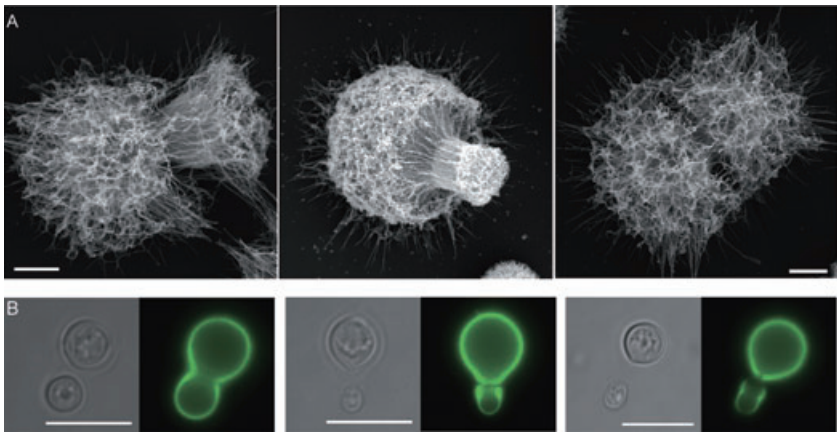

Fig. 9. Physical separation between the capsule of the mother cell and the bud.
A. Scanning EM of budding cells. Capsule growth and budding were induced as in Fig. 7. The cells were collected after 4 h of incubation in Sabouraud, and prepared for scanning EM as described in *Experimental procedures*. Scale bar, 2 microns. Three representative cells are shown.
B. Complement deposition in budding cells. Capsule growth was induced by placing the cells in the conditions described in the legend to Fig. 7, and C labelling was done by placing the cells in mouse serum for 1 h, followed by detection with immunofluorescence. Different pictures of budding cells in which the bud is at a different distance from the mother cell are shown (left, light microscopy; right, fluorescence). Scale bars, 10 μm.

growth. The mechanism of this Ab movement from cell-to-cell is not known, but we surmise that it reflects Ab dissociation, diffusion and re-association with its target antigen, as the concentration of antigen is changed by the addition of new unlabelled cells, and a new equilibrium established. Hence, as labelled and unlabelled cells are mixed, the mixture containing Ab comes to an equilibrium whereby Ab would distribute along the available epitopes as a function of accessibility and binding constant. Although this result makes sense from thermodynamic and equilibrium considerations, there are two peculiarities that should be addressed: redistribution does not result in homogenous staining of cells, and newly nascent buds are not stained. The absence of homogeneous binding may reflect that the system is not in full equilibrium after 24 h, or that binding is not intrinsically homogenous throughout the capsule. In this regard, mAbs to the GXM capsule can produce different fluorescence patterns and are not always uniform. This indicates that the epitope for each mAb is not uniformly distributed through the capsule. The absence of binding to the bud will be addressed later in the discussion.

In contrast to Ab, which binds antigen through non-covalent interactions such as salt-bridges, hydrophobic bonds, Van der Waal forces and hydrogen bonds, C binds to polysaccharide, and more particularly to GXM, by a thioester covalent bond (Kozel *et al*., 1984; 1989; 1992; Kozel and Pfrommer, 1986). As expected from its covalent interaction, we did not observe any exchange of fluorescence signal between C-labelled and unlabelled cells, supporting the potential usefulness of C labelling as a geographical marker during capsule growth. In addition, the binding of C to the capsule did not interfere with either capsule growth or cell replication. We also established that C was not binding to the yeast cell wall, as demonstrated by immunofluorescence where we stained the cell wall with calcofluor and the capsule with C. In this double staining experiment, C and calcofluor did not colocalize in encapsulated cells, a result in contrast to the results with the acapsular mutant, *cap67*, where C deposits in the cell wall, and provides a fluorescence pattern that almost colocalizes with calcofluor. In addition, we established that C bound to the capsule and not to the cell wall of encapsulated cells by showing that all C-binding could be removed by radiation, which is known to remove the capsule (Bryan *et al*., 2005). Furthermore, we established that C did not migrate to the capsule of newly generated buds. Taken together, these observations suggested that C was well suited to study the dynamics of capsule growth in *C. neoformans*, and to follow the fate of the capsule during replication. C localized to the inner regions of the capsule, in a location close to the cell wall. It is noteworthy that we did not observed C and mAb 18B7 colocalization in the capsule, with the Ab signal being always located more distally from the cell wall than the C signal. Concerning C localization, we believe that it is not found at the outer edge of the capsule because it can rapidly diffuse inside due to the lower density of the capsule at the outer edge (Gates *et al*., 2004). This location for C-binding may benefit the pathogen because it can interfere with C-mediated phagocytosis by placing C in a position where it does not interact with the complement receptor (CR) present in the phagocytic cells (Zaragoza *et al*., 2003b). However, in some conditions, C and mAb signals can colocalize. This occurs when the cells are first coated with mAb and then placed in serum. Under these conditions, the C localizes at the outer edge of the capsule (O. Zaragoza and A. Casadevall, submitted; Wang *et al*., 2005).

Using C as a marker of capsule location, we observed that C remained close to the cell wall after capsule growth. This result suggests that the capsule of *C. neoformans* grows by addition of new polysaccharide at the edge of the capsule. This observation is difficult to reconcile with the current model of capsule growth, which proposes enlargement by the addition of GXM to the inner region of the capsule, and the mixture of old and new polysaccharide at the outer edge of the capsule (Pierini and Doering, 2001). However, C has the potential limitation as a capsule marker that it does not bind to the outer edge of the capsule. Consequently we sought to validate our conclusions using a secondary method that did not involve either Ab or C labelling. Metabolic labelling of cells with induced capsule using ^{3}H-mannose revealed followed by graduated stripping of the capsule layers using γ-irradiation revealed highest specific activity near the capsule edge. This result confirms and validates the results obtained with the C labelling method. Our findings with C labelling imply a model of apical capsule growth whereby new polysaccharide migrates through the older capsular material to reach the capsular edge where it is assembled into the enlarging structure. According to our model, the C labelled region remains close to the cell wall during capsule growth, and may provide a backbone for the assembly of new polysaccharide to bind. As the molecular weight of soluble GXM is very high, being about 1.5×10^{6} Da (Gadebusch *et al*., 1964; Turner and Cherniak, 1991), and diffusion of such large molecules is difficult and unlikely to occur freely based on the dextran penetration studies (Gates *et al*., 2004), we suspect that smaller polysaccharide subunits travel through the older capsular material and reach the surface for assembly. Consistent with this scenario, analysis of capsule fractions has shown that much of the polysaccharide material in the capsule has low molecular mass (Bryan *et al*., 2005). Apical synthesis could also imply that the enzymatic machinery that catalyses the assembly of GXM is found at the edge of the capsule, or possibly throughout the capsule, but only active at the edge. At this point, we

cannot distinguish between these possibilities, but this model suggests that complex machinery is involved in capsule synthesis and its activity would change according to the area of the capsule.

Pierini and Doering presented other data that supported a capsule growth model in which the capsule grows by addition of the new polysaccharide in a location close to the cell wall. First, they noted that the area of the capsule more proximal to the cell wall became more compact after capsule growth. We believe that our model of capsule growth is also consistent with this interesting observation, because addition of new polysaccharide at the outer edge of the capsule could result in denser packing of the older polysaccharide. In addition, our model is also compatible with the idea that new fibres are intercalated into the pre-existing polysaccharide, which would also increase the density of this region, but the incorporation in this inner region does not necessarily imply displacement of the pre-existing polysaccharide. Second, pulse-chase experiments with radioactive xylose showed that this sugar was displaced to the outer edge of the capsule. However, the experimental conditions used for that particular experiment were not the same as the ones we used here. We cannot completely rule out that some polysaccharide is added in the inner part of the capsule, in a region distal to that where C binds, and would displace some polysaccharide to the outer edge.

We observed that when the cells were transferred several times to fresh inducing media there was not a significant increase in capsule size compared with the size of the capsule obtained after the first incubation in inducing medium. This implies that capsule growth and final size is a highly controlled process, and that the size of the capsule depends not only on the environment, but was also regulated by cellular factors. An uncontrolled capsule growth could have deleterious effects for the cells, because it could interfere with the proper separation of the bud from the mother cell, or even affect other cellular processes, like the capture of nutrients for the media. Furthermore, this observation suggests that *C. neoformans* cells have a mechanism to monitor the size of the capsule and to control it. It is known that GXM is produced and released to the medium continuously, so we do not think that a stop in capsule growth is the result of a cessation in the production of GXM. There could be several explanations to the stop of capsule growth, such as inability to attach the GXM at edge of the capsule, either by lack of the corresponding enzymatic activity, by the synthesis of a GXM with a different structure, or by the production of an inhibitory compound. The extent to which the capsule can grow is not known, but it is tempting to speculate that it depends on the size of the cell and of the bud that is going to emerge. In this regard, we have measured a positive correlation between capsule size and cell size (Fig. 5, Zaragoza *et al*., 2003a), which suggests the idea that capsule growth is a controlled process, and that factors that control cell size also control capsule size.

We also observed that once the capsule is built after incubation in inducing media, it does not decrease in size when placed in non-inducing medium again. This suggests that *C. neoformans* does not degrade the larger capsules after these are built, at least in the conditions studied. In fact, large cells remained in suspension while producing daughter cells with small capsules. This observation implies that the adaptation of cells with large capsule to new conditions, which produce cells with small capsules, occurs through the generation of new buds, which do not engage in large capsule growth. In this manner, the energetic cost of having a GXM degrading system could be invested in producing new cells.

The presence of a large capsule could potentially interfere with the separation of the bud from the mother cell. Hence, we investigated the dynamics of capsular rearrangements during budding and observed that when the capsule is large, there is an invagination at the capsule edge in the area where the bud is emerging. Immunofluorescence techniques revealed an opening in the capsule in the area of the bud, suggesting the formation of a tunnel at the site. If the capsule is linked to the cell wall, as has been suggested (Reese and Doering, 2003), rearrangements of the cell wall that precede bud formation could result in the release of GXM in that area.

In addition to the creation of a tunnel, it is likely that some force separates the bud from the mother cell after their cell walls separate. One hypothesis could be that rearrangements in the capsule and/or cell charge are responsible for providing the motive energy for the emergence of the bud. If this is true, it is reasonable to think that the capsule of the mother cell and the bud should not mix, to ensure the proper separation. Several observations in this study are consistent with such a scenario. First, we observed that when budding is induced in cells with big capsule that are growth arrested and labelled with either C or Ab, the signal of these markers never migrated to the bud, implying that the capsules do not mix (Figs 7 and 8). We also observed this phenomenon in our exchange experiment (see Fig. 1, panel A-VI). This observation is particularly interesting in the case of Ab labelling, because Ab can dissociate from the site of original binding and migrate between cells, observed both by fluorescence and FACS analysis. These results pose the fascinating observation that Ab can migrate from one cell to another, but not to the newly emerging bud. If this transfer occurred through direct contact of the cells, it would support a mechanism that blocks the exchange of capsule between the mother cells and the bud. If the Ab disassociated from the capsule was released to the medium, and then bound to unlabelled cells, this would imply that the new epitopes

of the bud cannot bind Abs at a low Ab concentration achievable in this experiment by dissociation of Ag–Ab complexes alone. Second, scanning EM revealed a chasm between the capsules of the mother and daughter cells, suggesting a physical separation. Third, scanning EM also showed that in the bud, the capsule synthesis must occur in a highly regulated manner, commencing from the tip away from the mother cell, and would grow at the same time as the bud arises, getting closer to the mother cells. The idea that capsule rearrangements and reorganization accounts for bud separation is consistent with our model of apical capsular growth. Capsule synthesis at the capsule edge in the bud could help separate the bud, a phenomenon that may not occur if the capsule was built in a location close to the cell wall. At this moment, we cannot discard that other factors, such as charge effects or localized pressure differences, also contribute to bud separation. In fact, it has been shown that the density of the capsule decreases at the outer edge, which could conceivably create a pressure gradient that facilitated the separation of the bud.

Based on our results, we propose here a new model for capsule growth in *C. neoformans* and for the rearrangements that occur in the capsule during budding. Our results are most easily interpreted as indicating that capsule growth occurs by addition of new polysaccharide to the edge of the existent capsule (Fig. 10A). According to our interpretation of the data, the region of the capsule close to the cell wall would not migrate to the edge, a model that is different from the previous model. Once the capsule is enlarged, transfer of cells to non-inducing medium does not result in a decrease of the capsule size, and new buds produced are adapted to the new conditions with a small capsule (Fig. 10B). During the process of budding, the capsule undergoes several rearrangements, involving the formation of a dimple in the capsule in the area of budding (Figs 6 and 10C). Also, a tunnel is formed (Figs 7, 8 and 10C, grey area), which allows the bud to travel through the capsule of the mother cell. During the process of budding, the bud begins to synthesize its own capsule (Figs 9A and 10, green in the model), beginning from the tip that is in the apical edge, related to the mother cell. As the mother and daughter cells separate, the capsule of the mother cells closes, allowing the efficient separation of the bud (see Fig. 7). Finally, when the cell walls separate and the bud is about to be release, the hole in capsule of the mother cell closes (Fig. 7A) and GXM is again found at the area of budding, because it is able to bind C again (see Fig. 9B). We note that this model of apical capsule growth is also supported by the recent observation that the polysaccharide made after capsule expansion *in vivo* is qualitatively different from that originally present in the cells (Charlier *et al.*, 2005). Although our model is different from that previously proposed (Pierini and Doering, 2001), we emphasize that we have no disagreement with the experimental data presented in the prior report, but rather differ in the interpretation of the results in light of evidence that Ag–Ab complexes in the capsule can dissociate and result in Ab redistribution. Furthermore, it is possible that some

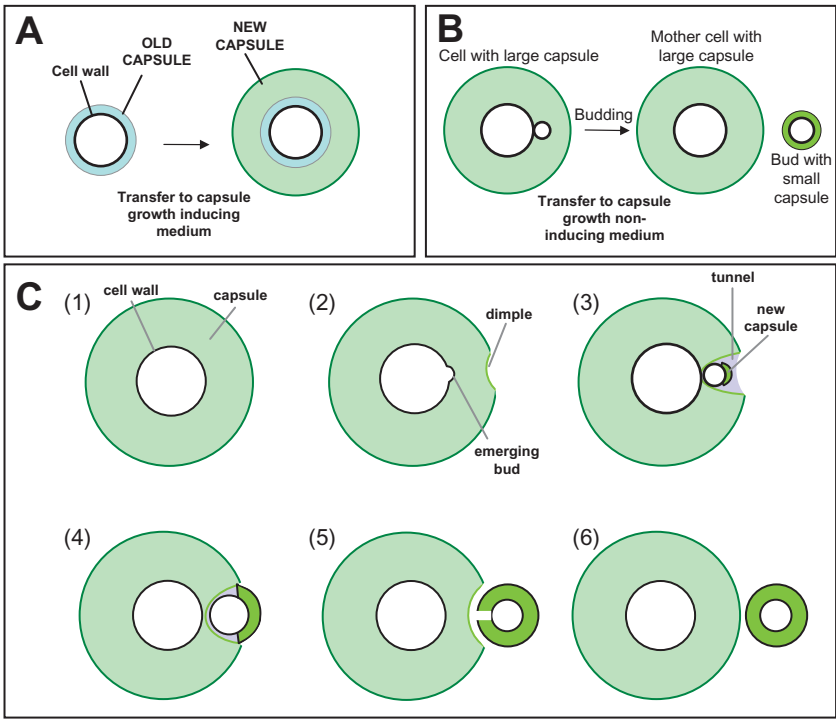

Fig. 10. Model of capsule growth and capsule rearrangements during budding in *C. neoformans*.
A. Model of capsule growth. After capsule enlarges newly synthesized capsule (light green) accumulates at the edge of the capsule, remaining the old capsule (light blue) close to the cell wall.
B. Model of adaptation to non-capsule growth inducing conditions. Cells with large capsules, when transferred to a medium that does not induce capsule growth, cannot degrade the capsule, but the new emerging buds have a small capsule.
C. Rearrangements of the capsule during budding. Panels 1–6 illustrate schematically different stages of budding. When bud arises, a dimple and a tunnel are formed (2, 3), which allows the separation of the bud. Bud growth is accompanied by capsule growth in the bud (3, 4). Capsule of the mother cell closes as the bud exits separates from the mother cell, at the same time that the bud completes the capsule without taking any polysaccharide of the mother cell (5), which will allow the complete separation of the bud (6).

aspects of each model are reconcilable. In this regard we cannot rule out that some portion of the capsule is added as proposed by the prior model. Beyond the difference between our models, we acknowledge the contribution of the previous work for it was the first study to capsule dynamics and put forth the questions that now define this field.

Experimental procedures

Yeast strains and growth conditions

Cryptococcus neoformans strain H99 (serotype A, Franzot *et al*., 1999), 24067 (serotype D, Jacobson and Tingler, 1994), 102.97 (serotype B, kindly provided by T. Mitchell, Durham, NC) and acapsular *cap67* mutant (Jacobson *et al*., 1982) were used in all studies. Yeast cells were grown overnight in Sabouraud medium at 30°C with moderate shaking (150 rpm). For capsule induction, two different protocols were used. The cells were washed with PBS, counted, and suspended in either 10% heat-inactivated fetal bovine serum (Gemini Bio-Products, Woodland, CA) (Zaragoza *et al*., 2003a), or diluted Sabouraud medium (1/10 dilution) in MOPS 50 mM pH 7.3 (Zaragoza and Casadevall, 2004). In both conditions, the cells were incubated overnight at 37°C. In these conditions average capsule enlarged from 2 to 10 μm (Zaragoza *et al*., 2003a; Zaragoza and Casadevall, 2004). For budding induction, the size of the capsule was induced for 3 days in the corresponding inducing medium (serum or diluted Sabouraud). In these conditions, the cells were arrested and not budding. They were then induced to replicate by placing in fresh inducing medium, or in Sabouraud media.

For the passage experiments, the size of the capsule size was induced for one night in inducing medium, and then the cells were placed at 2×10^6 cells per millilitre in fresh inducing medium for one night at 37°C. The size of the capsule was compared between cells that were passed to a new medium and cells that were maintained in the same medium for the same time.

Labelling of the capsule with either Ab or C and immunofluorescence

To label the capsule and follow capsule size during growth and budding, yeast cells were incubated with either mAb 18B7 or 2H1, which bind to the cryptococcal capsule (Casadevall *et al*., 1992a), or in 100 μl of mouse serum (freshly isolated) for 1 h at 37°C. In some experiments, mAb 2H1-Alexa 488 conjugated was used at 1 or 2 μg ml^{-1} (Feldmesser *et al*., 2000b). The cells were then washed twice with PBS, and placed in the corresponding medium. Localization of either C or Ab was observed by immunofluorescence, using fluorescein-isothiocynate (FITC) conjugated goat Ab to mouse C3 (5 μg ml^{-1}, Cappel) and/or goat anti-mouse IgG conjugated to tetramethyl-rhodamine-isothiocynate (TRITC) (Southern Biotechnology Associates, Birminghan, AL, 5 μg ml^{-1}). To detect the cell wall, calcofluor white (Sigma, MO) was added at this step at 50 μg ml^{-1}. After incubation for 1 h at 37°C, the cells were suspended in mounting medium (50% glycerol and 50 mM N-propyl gallate in PBS). Images were collected with an Olympus AX70 microscope, photographed with a QImaging Retiga 1300 digital camera using the QCapture Suite V2.46 software (QImaging, Burnaby BC, Canada), and processed with Adobe Photoshop 7.0 for Windows (San Jose, CA).

γ-irradiation of cryptococcal cells

γ-irradiation was used to release the cryptococcal capsule as described (Bryan *et al*., 2005). Cells from the wild-type (H99) and acapsular (cap67) strains were grown in Sabouraud, washed three times with PBS, and incubated in fresh mouse serum for 1 h at 37°C to allow C deposition. The cells were then washed, and suspended in PBS at a density of 10^7 cells per millilitre. Two millilitres of cell suspension were exposed to 137-Cs, which emanates γ-radiation at a constant dose rate of 14 Gy min^{-1} for 40 min. After irradiation, the presence of C was detected by immunofluorescence as described before.

Labelling of the capsule with ^{3}H-mannose and measuring radial incorporation of radioactivity

Cells from H99 strain were grown in Sabouraud medium overnight, and then placed in 2 ml of 50 mM MOPS buffer pH 7.3 in the presence of 50 μCi of ^{3}H-labelled mannose (Amersham, UK) at a concentration of 5×10^6 ml^{-1}. Parallel samples were prepared with the same amount of non-labelled mannose. The cells were then incubated for 3 h at 37°C, extensively washed with PBS, suspended in 1 ml of PBS, and the radioactivity incorporated into the cells was measured in a scintillation counter. The radioactivity present in the supernatant (initial background) was also measured. The cells were then irradiated for different times as described above and the radioactivity associated with cells and released into the supernatant was measured. The capsular polysaccharide released and the residual capsule size were measured in parallel in non-radioactive samples which had been subjected to the same radiation doses. Capsular polysaccharide was measured by capture enzyme-linked immunosorbent assay (ELISA; Casadevall *et al*., 1992b). Capsule size was calculated after visualization with Indian ink (see below). To calculate the ratio cpm per polysaccharide, both radioactivity and polysaccharide were measured, and the difference between irradiation times was calculated. From these values we calculated the amount of radioactivity incorporated into polysaccharide as a function of irradiation time. Supernatants from the irradiated cells were incubated with bromide-activated Sepharose (Sigma, St. Louis, MO) coupled to mAb to GXM (18B7) according with manufacturer's protocols and the radiation associated with the sepharose was then measured in a scintillation chamber.

Indian ink staining and capsule size measurement

Indian ink staining was done to measure capsule size in a protocol that involved 10 μl of a cell suspension with a drop of Indian ink on a slide. Images were obtained with the microscope described above, and the diameter of the whole

cell (capsule included) and cell body was measured with Adobe Photoshop. Capsule volume was calculated as the difference between the volume of the whole cell minus the volume of the cell body.

Ab exchange experiments

To evaluate whether Ab bound to one cell, dissociated, and then bound to another cell, we analysed stained and non-stained cells for redistribution of antibody to non-stained cells. For this experiment the size of the capsule was induced by incubation in serum as described. Then, 10^6 cells with enlarged capsule were labelled with either mAbs 18B7 or 2H1 (10 μg ml^{-1}) for 1 h at 37°C. In a parallel assay, the same number of cells with small capsule was suspended in PBS without antibody. The cells were then washed, and the last wash of the Ab-incubated cells was retained. Then, Ab-labelled and non-Ab-labelled cells were mixed in a 1:1 proportion in 100 μl of PBS, and incubated together overnight at 37°C. In some experiments, we labelled the cells with mAb 2HI conjugated to Alexa-488 (1 μg ml^{-1}). For negative controls, non-Ab-labelled cells (with small capsule) were suspended in the last wash of the Ab-incubated cells, and incubated overnight. The same protocol was carried out again; however, cells with small capsule were labelled with Ab, and cells with big capsule incubated with Ab were used as negative controls.

Ab exchange experiment analysed by FACS

Cells from H99 strain were grown overnight in Sabouraud medium at 30°C. The cells were washed with PBS three times and heat-killed by incubating them at 55°C for 30 min. Approximately 2×10^6 cells were suspended in 100 μl of PBS, mAb 2H1 conjugated to the fluorescent dye Alexa-488 was added at 1 or 2 μg ml^{-1}, and the cells were then incubated at 37°C for 1 h. The same number of cells was carried out in parallel without incubating with the mAb as negative control. The cells were then washed three times with PBS, the last wash of the mAb-coated cells was kept, and 2×10^6 unlabelled cells were incubated in this supernatant. The unlabelled and labelled cells were then incubated in 100 μl of PBS. This mixture of labelled and unlabelled cells was centrifuged and suspended in 10 ml of PBS. The samples were then incubated overnight at 37°C, suspended in 1 ml of PBS, and analysed on a Calibur FACscan flow cytometer (Becton Dickinson, Mountainview, CA) with CELLQuest (Becton Dickinson) and WinMDI 2.8 (Joeseph Trotter, La Jolla, CA). Each analysis evaluated 25 000 cells.

Isolation of RNA and real-time PCR protocol

Yeast cells were grown in Sabouraud medium overnight at 30°C, collected in the logarithmic phase of growth, transferred to capsule-inducing medium consisting of diluted Sabouraud (1/10 dilution) in MOPS buffer (50 mM pH 7.3) at a cell density of 10^7 ml^{-1}, and incubated at 37°C with moderate shaking for the times indicated. The cells were centrifuged and frozen at −20°C. Total RNA was isolated using the RNeasy Mini Kit (Qiagen, Valencia, CA) following the manufacturer's instructions. The purity and concentration of the total RNA was determined with an Agilent 2100 Bioanalyzer (Agilent Technologies, Palo Alto, CA). RNAs were treated with DNase I (Worthington, Lakewood, NJ) to eliminate potential DNA contamination. cDNA was made with the Superscript II kit (Invitrogen, Carlsbad, CA) following the manufacturer's instructions. Parallel samples without reverse transcriptase (RT^-) were prepared as control. Real-time PCR was performed in 384 well Clean Optical Reaction Plates (Applied Biosystem), each well containing 4 μl of SYBRgreen PCR Master Mix (Applied Biosystem, Warrington, UK), 2 μl of cDNA and 2 μl of a pair of oligonucleotides specifics for each gene (500 nM final concentration). The PCR was performed in an ABI Prism® 7900 HT Sequence Detection System using the following cycles: 10 s at 95°C, 90 s at 60°C and 30 s at 72°C. This cycle was repeated 40 times. The results were analysed with the SDS 2.0 software (Applied Biosystem), and the Ct values were exported to Excel for windows XP, where the relative changes were calculated and plotted. The mRNA levels of the housekeeping gene encoding glyceraldehide-3P dehydrogenase (GAPDH) were measured and used to normalize the data. The following primers were used in the real-time PCR: *CAP10* (AGGTCATTTCTTCTCCGATTG and ATGTCGCTGTATCCCATACTC), *CAP59* (TCCGATCCACA GGACAGGAG and TCTGGTCCGGGGACAAACTC), *CAP60* (GGCAGCCAAATCTAATTCCA and CAGAAGCTCTGGAAT GGGAG), *CAP64* (AAAGACGGCTACCTTTCAAGA and GTCCTTGATTAGCTCTGCCC) and GAPDH (CTTCCCACA AGGACTGGC and CTTCCCACAAGGACTGGC).

Scanning EM

Yeast cells were washed with PBS and suspended in fixing solution (2% p-formaldehyde, 2.5% glutaraldehyde and 0.1 M sodium cacolydate) until analysed. The cells were then serially dehydrated with increasing concentrations of ethanol, dried and coated with gold palladium (Desk-1; Denton Vacuum, Cherry Hill, NJ). Finally, they were visualized with a JEOL (Tokyo, Japan) JAM-6400 electron microscope.

Statistics

T-tests were used to compare differences between groups, and correlation coefficient was obtained with Pearson Test. All the statistics were performed with the Unistat 5.5 (Unistat, London, England). Significant differences were considered when the *P*-value was below 0.05.

Acknowledgements

We thank Drs June Kwon Chung, J. Perfect, T. Mitchell for the gift of strains, Irene Puga and Dr F. Macián for help with FACS experiments, Dr J. Zavadil and Dona Wu for help with the real-time PCR technique, and Dr Johanna Rivera for the gift of mAb 2H1 conjugated to Alexa 488, and Dr M. Rodrigues for Sepharose conjugated to mAb 18B7. We thank Diane McFadden for useful conversations, ideas and critical reading of the manuscript. Arturo Casadevall is supported by the following grants: AI33774-11, HL59842-07, AI33142-11, AI52733-02, GM07142-01.

References

Bar-Peled, M., Griffith, C.L., and Doering, T.L. (2001) Functional cloning and characterization of a UDP-glucuronic acid decarboxylase: the pathogenic fungus *Cryptococcus neoformans* elucidates UDP-xylose synthesis. *Proc Natl Acad Sci USA* **98:** 12003–12008.

Bar-Peled, M., Griffith, C.L., Ory, J.J., and Doering, T.L. (2004) Biosynthesis of UDP-GlcA, a key metabolite for capsular polysaccharide synthesis in the pathogenic fungus *Cryptococcus neoformans*. *Biochem J* **381:** 131–136.

Bergman, F. (1965) Studies on capsule synthesis of *Cryptococcus neoformans*. *Sabouraudia* **4:** 23–31.

Bose, I., Reese, A.J., Ory, J.J., Janbon, G., and Doering, T.L. (2003) A yeast under cover: the capsule of *Cryptococcus neoformans*. *Eukaryot Cell* **2:** 655–663.

Bryan, R.A., Zaragoza, O., Zhang, T., Ortiz, G., Casadevall, A., and Dadachova, E. (2005) Radiological studies reveal radial differences in the architecture of the polysaccharide capsule of *Cryptococcus neoformans*. *Eukaryot Cell* **4:** 465–475.

Casadevall, A., and Perfect, J.R. (1998) *Cryptococcus Neoformans.* Washington, DC: American Society for Microbiology Press.

Casadevall, A., Mukherjee, J., Devi, S.J., Schneerson, R., Robbins, J.B., and Scharff, M.D. (1992a) Antibodies elicited by a *Cryptococcus neoformans*-tetanus toxoid conjugate vaccine have the same specificity as those elicited in infection. *J Infect Dis* **165:** 1086–1093.

Casadevall, A., Mukherjee, J., and Scharff, M.D. (1992b) Monoclonal antibody based ELISAs for cryptococcal polysaccharide. *J Immunol Methods* **154:** 27–35.

Chang, Y.C., and Kwon-Chung, K.J. (1994) Complementation of a capsule-deficient mutation of *Cryptococcus neoformans* restores its virulence. *Mol Cell Biol* **14:** 4912–4919.

Chang, Y.C., and Kwon-Chung, K.J. (1998) Isolation of the third capsule-associated gene, CAP60, required for virulence in *Cryptococcus neoformans*. *Infect Immun* **66:** 2230–2236.

Chang, Y.C., and Kwon-Chung, K.J. (1999) Isolation, characterization, and localization of a capsule-associated gene, CAP10, of *Cryptococcus neoformans*. *J Bacteriol* **181:** 5636–5643.

Chang, Y.C., Penoyer, L.A., and Kwon-Chung, K.J. (1996) The second capsule gene of *Cryptococcus neoformans*, CAP64, is essential for virulence. *Infect Immun* **64:** 1977–1983.

Charlier, C., Chretien, F., Baudrimont, M., Mordelet, E., Lortholary, O., and Dromer, F. (2005) Capsule structure changes associated with *Cryptococcus neoformans* crossing of the blood–brain barrier. *Am J Pathol* **166:** 421–432.

Cherniak, R., and Sundstrom, J.B. (1994) Polysaccharide antigens of the capsule of *Cryptocccus neoformans*. *Infect Immun* **62:** 1507–1512.

Cherniak, R., O'Neill, E.B., and Sheng, S. (1998) Assimilation of xylose, mannose, and mannitol for synthesis of glucuronoxylomannan of *Cryptococcus neoformans* determined by 13C nuclear magnetic resonance spectroscopy. *Infect Immun* **66:** 2996–2998.

Cruickshank, J.G., Cavill, R., and Jelbert, M. (1973) *Cryptococcus neoformans* of unusual morphology. *Appl Microbiol* **25:** 309–312.

Doering, T.L. (2000) How does Cryptococcus get its coat? *Trends Microbiol* **8:** 547–553.

Feldmesser, M., Kress, Y., Novikoff, P., and Casadevall, A. (2000a) *Cryptococcus neoformans* is a facultative intracellular pathogen in murine pulmonary infection. *Infect Immun* **68:** 4225–4237.

Feldmesser, M., Rivera, J., Kress, Y., Kozel, T.R., and Casadevall, A. (2000b) Antibody interactions with the capsule of *Cryptococcus neoformans*. *Infect Immun* **68:** 3642–3650.

Feldmesser, M., Kress, Y., and Casadevall, A. (2001) Dynamic changes in the morphology of *Cryptococcus neoformans* during murine pulmonary infection. *Microbiology* **147:** 2355–2365.

Franzot, S.P., Salkin, I.F., and Casadevall, A. (1999) *Cryptococcus neoformans* var. *grubii*: separate varietal status for *Cryptococcus neoformans* serotype A isolates. *J Clin Microbiol* **37:** 838–840.

Gadebusch, H.H., Ward, P.A., and Frenkel, E.P. (1964) Natural host resistance to infection with *Cryptococcus Neoformans*. III. The effect of cryptococcal polysaccharide upon the physiology of the reticuloendothelial system of laboratory animals. *J Infect Dis* **114:** 95–106.

Garcia-Rivera, J., Chang, Y.C., Kwon-Chung, K.J., and Casadevall, A. (2004) *Cryptococcus neoformans* CAP59 (or Cap59p) is involved in the extracellular trafficking of capsular glucuronoxylomannan. *Eukaryot Cell* **3:** 385–392.

Gates, M.A., Thorkildson, P., and Kozel, T.R. (2004) Molecular architecture of the *Cryptococcus neoformans* capsule. *Mol Microbiol* **52:** 13–24.

Granger, D.L., Perfect, J.R., and Durack, D.T. (1985) Virulence of *Cryptococcus neoformans*. Regulation of capsule synthesis by carbon dioxide. *J Clin Invest* **76:** 508–516.

Jacobson, E.S., and Tingler, M.J. (1994) Strains of *Cryptococcus neoformans* with defined capsular phenotypes. *J Med Vet Mycol* **32:** 401–404.

Jacobson, E.S., Ayers, D.J., Harrell, A.C., and Nicholas, C.C. (1982) Genetic and phenotypic characterization of capsule mutants of *Cryptococcus neoformans*. *J Bacteriol* **150:** 1292–1296.

Kozel, T.R., and Gotschlich, E.C. (1982) The capsule of *Cryptococcus neoformans* passively inhibits phagocytosis of the yeast by macrophages. *J Immunol* **129:** 1675–1680.

Kozel, T.R., and Pfrommer, G.S. (1986) Activation of the complement system by *Cryptococcus neoformans* leads to binding of iC3b to the yeast. *Infect Immun* **52:** 1–5.

Kozel, T.R., Gulley, W.F., and Cazin, J., Jr (1977) Immune response to *Cryptococcus neoformans* soluble polysaccharide: immunological unresponsiveness. *Infect Immun* **18:** 701–707.

Kozel, T.R., Highison, B., and Stratton, C.J. (1984) Localization on encapsulated *Cryptococcus neoformans* of serum components opsonic for phagocytosis by macrophages and neutrophils. *Infect Immun* **43:** 574–579.

Kozel, T.R., Pfrommer, G.S., Guerlain, A.S., Highison, B.A., and Highison, G.J. (1988) Role of the capsule in phagocytosis of *Cryptococcus neoformans*. *Rev Infect Dis* **10** (Suppl. 2)**:** S436–S439.

Kozel, T.R., Wilson, M.A., Pfrommer, G.S., and Schlageter,

A.M. (1989) Activation and binding of opsonic fragments of C3 on encapsulated *Cryptococcus neoformans* by using an alternative complement pathway reconstituted from six isolated proteins. *Infect Immun* **57:** 1922–1927.

Kozel, T.R., Wilson, M.A., and Welch, W.H. (1992) Kinetic analysis of the amplification phase for activation and binding of C3 to encapsulated and nonencapsulated *Cryptococcus neoformans*. *Infect Immun* **60:** 3122–3127.

Kozel, T.R., Levitz, S.M., Dromer, F., Gates, M.A., Thorkildson, P., and Janbon, G. (2003) Antigenic and biological characteristics of mutant strains of *Cryptococcus neoformans* lacking capsular O acetylation or xylosyl side chains. *Infect Immun* **71:** 2868–2875.

Love, G.L., Boyd, G.D., and Greer, D.L. (1985) Large *Cryptococcus neoformans* isolated from brain abscess. *J Clin Microbiol* **22:** 1068–1070.

McFadden, D.C., and Casadevall, A. (2004) Unexpected diversity in the fine specificity of monoclonal antibodies that use the same V region gene to glucuronoxylomannan of *Cryptococcus neoformans*. *J Immunol* **172:** 3670–3677.

Mitchell, T.G., and Friedman, L. (1972) *In vitro* phagocytosis and intracellular fate of variously encapsulated strains of *Cryptococcus neoformans*. *Infect Immun* **5:** 491–498.

Moyrand, F., Klaproth, B., Himmelreich, U., Dromer, F., and Janbon, G. (2002) Isolation and characterization of capsule structure mutant strains of *Cryptococcus neoformans*. *Mol Microbiol* **45:** 837–849.

Mukherjee, J., Casadevall, A., and Scharff, M.D. (1993) Molecular characterization of the humoral responses to *Cryptococcus neoformans* infection and glucuronoxylomannan-tetanus toxoid conjugate immunization. *J Exp Med* **177:** 1105–1116.

Murphy, J.W., and Cozad, G.C. (1972) Immunological unresponsiveness induced by cryptococcal capsular polysaccharide assayed by the hemolytic plaque technique. *Infect Immun* **5:** 896–901.

Pierini, L.M., and Doering, T.L. (2001) Spatial and temporal sequence of capsule construction in *Cryptococcus neoformans*. *Mol Microbiol* **41:** 105–115.

Reese, A.J., and Doering, T.L. (2003) Cell wall alpha-1,3-glucan is required to anchor the *Cryptococcus neoformans* capsule. *Mol Microbiol* **50:** 1401–1409.

Rivera, J., Feldmesser, M., Cammer, M., and Casadevall, A. (1998) Organ-dependent variation of capsule thickness in *Cryptococcus neoformans* during experimental murine infection. *Infect Immun* **66:** 5027–5030.

Sommer, U., Liu, H., and Doering, T.L. (2003) An alpha-1,3-mannosyltransferase of *Cryptococcus neoformans*. *J Biol Chem* **278:** 47724–47730.

Steenbergen, J.N., Shuman, H.A., and Casadevall, A. (2001) *Cryptococcus neoformans* interactions with amoebae suggest an explanation for its virulence and intracellular pathogenic strategy in macrophages. *Proc Natl Acad Sci USA* **98:** 15245–15250.

Tucker, S.C., and Casadevall, A. (2002) Replication of *Cryptococcus neoformans* in macrophages is accompanied by phagosomal permeabilization and accumulation of vesicles containing polysaccharide in the cytoplasm. *Proc Natl Acad Sci USA* **99:** 3165–3170.

Turner, S.H., and Cherniak, R. (1991) Glucuronoxylomannan of *Cryptococcus neoformans* serotype B: structural analysis by gas-liquid chromatography-mass spectrometry and 13C-nuclear magnetic resonance spectroscopy. *Carbohydr Res* **211:** 103–116.

Vartivarian, S.E., Anaissie, E.J., Cowart, R.E., Sprigg, H.A., Tingler, M.J., and Jacobson, E.S. (1993) Regulation of cryptococcal capsular polysaccharide by iron. *J Infect Dis* **167:** 186–190.

Vecchiarelli, A. (2000) Immunoregulation by capsular components of *Cryptococcus neoformans*. *Med Mycol* **38:** 407–417.

Wang, F., Nakouzi, A., Alvarez, M., Zaragoza, O., Angeletti, R.H., and Casadevall, A. (2005) Structural and functional characterization of glycosylation in an immunoglobulin G1 to *Cryptococcus neoformans* glucuronoxylomannan. *Mol Immunol* (in press).

Zaragoza, O., and Casadevall, A. (2004) Experimental modulation of capsule size in *Cryptococcus neoformans*. *Biol Proced Online* **6:** 10–15.

Zaragoza, O., Fries, B.C., and Casadevall, A. (2003a) Induction of capsule growth in *Cryptococcus neoformans* by mammalian serum and CO(2). *Infect Immun* **71:** 6155–6164.

Zaragoza, O., Taborda, C.P., and Casadevall, A. (2003b) The efficacy of complement-mediated phagocytosis of *Cryptococcus neoformans* is dependent on the location of C3 in the polysaccharide capsule and involves both direct and indirect C3-mediated interactions. *Eur J Immunol* **33:** 1957–1967.

